Bull. Astr. Soc. India (1996) **24**, 321–324

Seismology of the solar core

H. M. Antia and S. M. Chitre

Tata Institute of Fundamental Research, Homi Bhabha Road, Bombay 400 005, India

Abstract. The accurately observed solar *p*-mode frequencies are employed to constrain the temperature and chemical composition profiles in the solar core. An iterative procedure is adopted to perform a primary inversion of the helioseismic data, using the mechanical constraints to obtain the variation of density and sound speed in the solar interior. The secondary inversion adopts the equations of thermal equilibrium, with the additional constraints such as the equation of state, the opacity, the nuclear energy generation rate and the observed solar luminosity for deriving the temperature and chemical composition profiles in the solar core. The iterative technique can be effectively applied to infer the radial as well as latitudinal variation of the Sun's rotation rate from the observed rotational splittings. It turns out that the observed surface differential rotation persists through the solar convection zone, while the solar core appears to rotate slower than the equatorial regions at the solar surface.

Key words: Sun: Oscillations, Sun: Interior, Sun: Rotation

1. Iterated seismic model

With the help of the observed frequencies from the BBSO data (Libbrecht et al. 1990) combined with the low degree modes from Jiménez et al. (1988), BISON (Elsworth et al. 1994), IRIS (Gelly et al. 1994) or IPHIR (Toutain & Fröhlich 1992), we infer the sound speed and density in the solar interior using a non-asymptotic inversion technique (Antia & Basu 1994, Antia 1995) based on the variational principle. Adopting a reference solar model, we compute the sound speed and density in the Sun using the frequency difference between the observed frequencies and the computed frequencies for the reference solar model. This seismic model is iteratively refined by computing the eigenfrequencies for the seismic model and comparing them with the observed frequencies (cf., Antia 1995). The iterative process is continued until a suitable convergence criterion is satisfied.

The results are shown in Figure 1, which shows the relative difference in sound speed and density between the seismic solar models and the standard solar model of Bahcall and

Pinsonneault (1995) (hereinafter BP) which includes the diffusion of helium and heavy elements. It can be seen that in general the sound speed and density in the standard solar model are fairly close to those in the seismic models. Most significant deviation arises in the convection zone, which is very likely due to the equation of state adopted by BP in constructing the solar model. This difference is significantly reduced if the solar model is constructed with a better equation of state (Antia 1995).

Apart from this there is a significant discrepancy near the base of the convection zone, which could arise due to either incorrect depth of convection zone or adoption of an incorrect composition profile just below the convection zone. It turns out that the hydrogen abundance X has a sharp dip just below the base of the convection zone on account of diffusion in the model of BP. It is conceivable that in the Sun this dip is not as sharp as that in the model (Basu and Antia 1994).

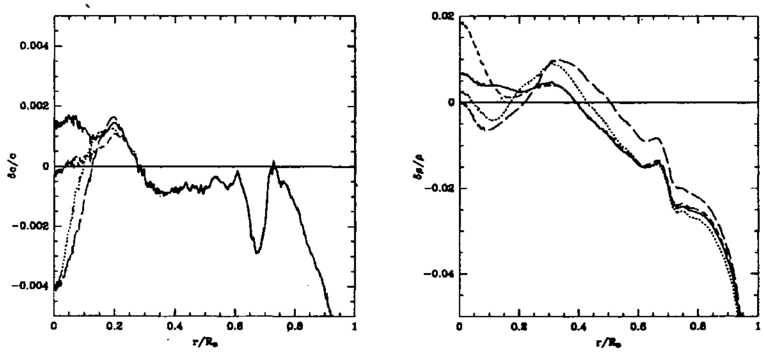

Figure 1. Relative sound speed and density difference between the standard solar model of BP and the seismic models (in the sense BP − seismic model). The seismic models differ in the low degree data that is used for inversion. The solid line represents results using BISON data, the dotted line shows results using IRIS data, the short dashed line shows the results using data from Jiménez et al. (1988), while the long dashed line shows the results using IPHIR data.

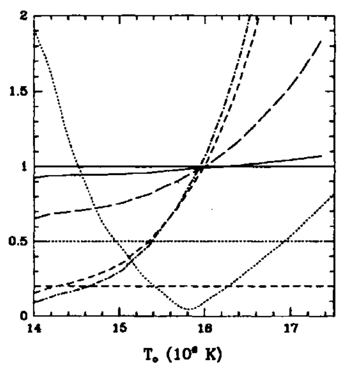

Figure 2. The neutrino fluxes and luminosity as a function of central temperature. The continuous curve shows the luminosity, while the neutrino fluxes are displayed by the short dashed curve (^{37}Cl detector), long dashed curve (^{71}Ga detector) and dot short dashed curve (^{8}B neutrinos). All these quantities are scaled with respect to the value in the standard solar model of BP. The dotted curve shows the extent by which the opacity needs to be modified.

2. Inversion for thermal structure

With the density and sound speed obtained from the seismic solar models we perform a secondary inversion to infer the temperature and helium abundance profiles in the solar core ($r \leq 0.3R_\odot$) with the help of the equations of thermal equilibrium (Antia & Chitre 1995). The secondary inversion also requires physical inputs like the equation of state, the opacity and the nuclear energy generation rate. In this work we have adopted the MHD (Hummer & Mihalas 1988; Mihalas, Däppen & Hummer 1988; Däppen et al. 1988) equation of state, the OPAL opacity (Rogers & Iglesias 1992) and nuclear energy generation rate as given by Bahcall (1989). For a given central temperature we choose the temperature profile in the solar core that minimizes the extent to which opacities have to be modified as compared to the OPAL values. In general, the computed total energy generation inside the solar core does not yield the observed solar luminosity and we adjust the nuclear reaction rate by just multiplying the computed rate with a constant factor to yield the correct luminosity. The results for the seismic solar model using the BBSO+BISON frequencies are shown in Figure 2. It can be seen that the opacity modification is minimum at a central temperature of $\approx 15.8 \times 10^6$ K, which is thus the preferred central temperature with the current input physics. The computed luminosity (before applying correction to the nuclear energy generation rates) at this central temperature is $0.98 L_\odot$.

It should be noted that in these results we have used the nuclear reaction rates as given by Bahcall (1989) which have later been revised by Kamionkowski and Bahcall (1994a,b). The revised cross-section for the pp reaction is about 5% lower, which gives much lower solar luminosity for the computed seismic models. In fact, with the revised nuclear reaction rates it is not possible to find a temperature profile for which the computed luminosity is within 1% of the observed solar luminosity and the required opacity modification for realizing the temperature profile is less than 20%. Thus, it appears that the revised nuclear reaction rates are not consistent with seismic models, though the difference between different seismic models is of the same order as the discrepancy. Hopefully, the better (more accurate) helioseismic data that is likely to be available in near future will enable us to estimate the uncertainties in the nuclear reaction rates more reliably.

3. Internal rotation profile

The technique of iterative refinement is also useful for determining the rotation profile inside the Sun (Antia et al. (1996)). In order to determine the latitudinal dependence of the rotation rate, we follow Ritzwoller and Lavely (1991) and express the rotation rate as

$$v_{\rm rot}(r,\theta) = \Omega(r,\theta) r \sin\theta = -\sum_{s=0}^{\infty} w_{2s+1}^0(r) \frac{\partial}{\partial\theta} Y_{2s+1}^0(\theta), \qquad (1)$$

where θ is the colatitude and $w_s(r)$ are expansion coefficients which need to be determined by inversion, using the observed splitting coefficients as shown by Ritzwoller and Lavely (1991). The individual components $w_1(r)$, $w_3(r)$ and $w_5(r)$ are calculated by solving separate one-dimensional inversion problem with the iterative refinement of the regularized least squares solution. The observed rotational splitting coefficients from BBSO observations (Woodard & Libbrecht 1993) are used for $l \geq 5$, while for low degree we employ the recent rotational splittings from BISON (Elsworth et al 1995). The results are displayed in Figures 3–5.

It is clear that the surface differential rotation persists through the solar convection zone, while below the base of convection zone the rotation rate appears to be relatively independent of latitude. The transition at the base of the convection zone may not be resolved by the observed data on splittings. Finally, the core appears to be rotating slower than the surface equatorial rotation rate as found by Tomczyk et al. (1995) and Elsworth et al. (1995).

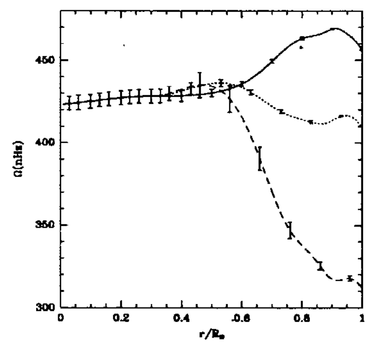

Figure 3. The rotation rate as a function of radial distance at the equator (solid line), pole (dashed line) and 45° latitude (dotted line).

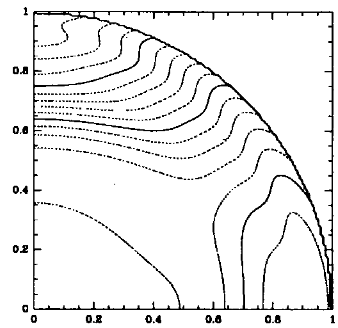

Figure 4. The diagram showing contours of constant rotation rate. The horizontal axis is the equator, while the vertical axis represents the pole. The solid lines represent contours with rotation rate in multiples of 50 nHz, while the dotted lines represent contours with interval of 10 nHz. The outermost contour is for $\Omega = 460$ nHz.

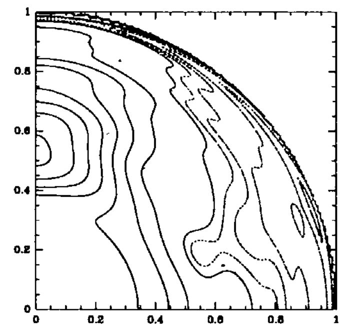

Figure 5. The diagram showing contours of constant errors in the inverted rotation rate. The horizontal axis is the equator, while the vertical axis represents the pole. The solid lines represent contours with errors in multiples of 1 nHz, starting with 1 nHz at the rightmost contour. The dotted lines represent contours with interval of 0.2 nHz, while the outermost contour is for an error of 0.1 nHz.

References

Antia, H. M. 1995, A&A (in press).

Antia, H. M. & Basu, S. 1994, A&AS 107, 421.

Antia, H. M. & Chitre, S. M. 1995, ApJ 442, 434.

Antia, H. M., Chitre, S. M. & Thompson, M. J. 1996, A&A (in press).

Basu, S., Antia, H. M. 1994, MNRAS, 269, 1137.

Bahcall, J. N. 1989, Neutrino Astrophysics, (Cambridge: Cambridge Univ. Press).

Bahcall, J. N. & Pinsonneault, M. H. 1995, Rev. Mod. Phys. (in press).

Däppen, W., Mihalas, D., Hummer, D. G. & Mihalas, B. W. 1988, ApJ 332, 261.

Elsworth, Y., Howe, R., Isaak, G. R., McLeod, C. P., Miller, B. A., New, R., Speake, C. C. & Wheeler, S. J. 1994, ApJ 434 801.

Elsworth, Y., Howe, R., Isaak, G. R., McLeod, C. P., Miller, B. A., New, R., Wheeler, S. J. & Gough, D. O. 1995, Nature 376, 669.

Gelly et al. 1994, in Highlights of Astronomy, 10 (in press).

Hummer, D. G., Mihalas, D. 1988, ApJ 331, 794.

Jiménez, A., Pallé, P. L., Pérez, J. C., Régulo, C., Roca-Cortés, T., Isaak, G. R., McLeod, C. P. van der Raay, H. 1988, in Advances in Helio- and Asteroseismology: Proc. IAU Symp. 123, eds. J. Christensen-Dalsgaard, S. Frandsen (Dordrecht: D. Reidel) p205.

Kamionkowski, M. & Bahcall, J. N. 1994a, ApJ 331, 794.

Kamionkowski, M. & Bahcall, J. N. 1994b, Phys. Rev. C49, 545.

Libbrecht, K. G., Woodard, M. F., Kaufman, J. M. 1990, ApJS 74, 1129.

Mihalas, D., Däppen, W., Hummer, D. G. 1988, ApJ 331, 815.

Ritzwoller, M. H., Lavely, E. M., 1991, ApJ 369, 557.

Rogers, F. J., Iglesias, C. A. 1992, ApJS 79, 507.

Tomczyk, S., Schou, J. & Thompson, M. J. 199˜ ApJ 448, L57.

Toutain, T. & Fröhlich, C., 1992, A&A, 257, 28

Woodard, M. F., Libbrecht, K. G., 1993, ApJ 402, L77.